Jets as a Source of Information About Photon Structure

Marek Taševský
Institute of Physics, AS CR, Na Slovance 2,
Praha, 180 00, Czech Republic
E-mail: tasevsky@mail.desy.de

(representing the H1 Collaboration)

A review of recent jet measurements of the photon structure from the H1 experiment at HERA is presented. The scale and the virtuality dependence of the effective parton distribution function of the photon is discussed.

1 Introduction

The photon, as an elementary particle, is considered to be structureless. And yet, from numerous experimental data it follows that in high energy $\gamma\gamma$ or γp interactions the photon behaves like a hadron, an object with a structure. Quantum mechanically, the photon can fluctuate into a fermion-antifermion pair which can further evolve in the framework of QED and QCD. This is called photon structure and it can be investigated by means of the jets. Like those of the proton, parton distribution functions (PDF) of the photon depend on the probing scale[1], but additionally also on its virtuality Q^2. This latter dependence was measured in the single-jet study [2] and more recently in an H1 di-jet analysis where the effective PDF of the virtual photon was extracted for the first time.

2 Single-Jet and Di-Jet Cross Sections

In ep collisions the resolved photon contribution to the di-jet cross-section is

$$\frac{\mathrm{d}\sigma^{\mathrm{ep}}}{\mathrm{d}y\mathrm{d}x_\gamma\mathrm{d}x_p\mathrm{d}\cos\theta\mathrm{d}Q^2} = \frac{f_{\gamma/e}(y,Q^2)}{y}\sum_{i,j,k,l}\frac{f_{i/\gamma}(x_\gamma,\mu_F^2,Q^2)}{x_\gamma}\frac{f_{j/p}(x_p,\mu_F^2)}{x_p}|M_{ij}^{kl}|^2 \tag{1}$$

where $f_{\gamma/e}$ denotes the flux of transversely polarised virtual photons inside electron, $f_{i/\gamma}$, $f_{j/p}$ are PDF of the photon and proton respectively, taken at the factorization scale μ_F, and M_{ij}^{kl} are the leading order (LO) matrix elements of the binary parton level processes $ij \to kl$, proportional to $\alpha_s(\mu_R^2)$. We assumed $\mu_F = \mu_R = E_T$.

To correct for detector, fragmentation and higher order effects, PYTHIA and HERWIG MC event generators were used for photoproduction and HER-

WIG, RAPGAP, ARIADNE and LEPTO for low Q^2 events. As input PDFs of the virtual photon, either the simple Drees-Godbole [3] (DG) virtuality suppression factor $L(E_T^2, Q^2, \omega)$ multiplying the PDFs of the real photon (as L for quarks and L^2 for gluons) [a] or set D of the SaS[4] parametrisations was taken.

In Fig.1a the photoproduction di-jet cross sections are compared with next-to-leading order (NLO) calculations in which the photon PDFs were taken from F_2^γ measurements in $\gamma\gamma$ interactions at LEP. The satisfactory overall description of the di-jet ep data supports the universality of the photon parton distributions. However, the data indicate that adjustments of the PDF at high x_γ are required where no F_2^γ measurements have been made so far.

In Fig.1b the inclusive single-jet cross sections as a function of Q^2 are compared to predictions of LEPTO which contains only the direct coupling of the photon to quarks. The prediction agrees with the data well in the DIS region where, typically, $E_T^2 \ll Q^2$. However, the model cannot describe the data in the region $E_T^2 > Q^2$ where the contribution of the virtual resolved photon is expected to be important. If the same data are compared to HERWIG and RAPGAP, generators containing resolved processes, a good agreement is achieved only if the photon PDF is suppressed with increasing Q^2 [2]. The virtuality dependence of the di-jet cross sections, $\mathrm{d}\sigma/\mathrm{dx}_\gamma$, is shown in Fig.2. Again, the HERWIG and RAPGAP models incorporating a resolved photon contribution with a virtuality-dependent suppression, describe the data satisfactorily. In Fig.3a, the ratio of resolved to direct contributions, defined as $\sigma(x_\gamma \leq 0.75)/\sigma(x_\gamma > 0.75)$ is plotted as a function of Q^2. The data in Figs. 2 and 3a are compatible with DG virtuality suppression for $0.05 \leq \omega \leq 0.1$ GeV.

3 Effective Parton Distribution of the Photon

The concept of effective PDF was developed for jet analyses at CERN SPS [5] where it was not possible to distinguish the contributions of individual subprocesses $ij \to kl$ to the sum in Eq. (1). Applied to ep collisions at HERA, this approach allows us to approximate the formula (1) by a simple product

$$\frac{\mathrm{d}\sigma^{ep}}{\mathrm{d}y\mathrm{d}x_\gamma \mathrm{d}x_p \mathrm{d}cos\theta \mathrm{d}Q^2} \approx \frac{f_{\gamma/e}(y,Q^2)}{y}\frac{f_{\mathrm{eff}}^\gamma(x_\gamma,E_T^2,Q^2)}{x_\gamma}\frac{f_{\mathrm{eff}}^p(x_p,E_T^2)}{x_p}|M_{SES}|^2 \quad (2)$$

of a *single effective subprocess* matrix element M_{SES} and the *effective PDF* of the colliding photon and proton $f_{\mathrm{eff}} = \sum[q_i + \overline{q}_i] + \frac{9}{4}g$ (sum over all quark flavours). The measured di-jet cross sections were corrected to the LO di-parton cross section by an unfolding procedure [6]. The effective PDF of the

[a] $L(E_T^2, Q^2, \omega) = \frac{\ln((E_T^2+\omega^2)/(Q^2+\omega^2))}{\ln((E_T^2+\omega^2)/\omega^2)}$, with ω being a free parameter

photon $f_{\rm eff}^{\gamma}$ was determined by comparing the measured di-parton cross section with that calculated by MC model using the GRV-LO photon PDF and incorporating, for the virtual photon, the DG suppression factor.

In Figure 3b the effective PDF of the (almost) real photon integrated over the range $0.4 < x_\gamma < 0.7$ is shown as a function of the scale E_T^2. In this x_γ region $f_{\rm eff}^{\gamma}$ is dominated by the quarks. Also shown are the PDFs from GRV-LO parametrizations of the photon [7], which is in good agreement with the data, and of the pion [8], which differs from measurement both in shape and absolute rate. The increase of $f_{\rm eff}^{\gamma}$ with E_T^2 seen in the data is compatible with a logarithmic dependence of q^γ on μ_F, which is expected from the inhomogenous term in the DGLAP evolution equation. In Fig. 4 the effective PDF of the virtual photon is presented in four Q^2 intervals and compared with the predictions of GRV–LO (for $\omega = 0.05$ and 0.1 GeV) and with SaS1D and SaS2D parametrizations. The data are in good agreement with the GRV for both values of ω, the SaS parametrisations tend to fall more rapidly in the low x_γ region than the data.

4 Conclusion

New kinematical regions were explored by the H1 experiment in single-jet and di-jet analyses. From photoproduction data the scale dependence of the photon effective PDF was determined. The observed logarithmic increase agrees with the prediction of perturbative QCD. The low Q^2 data indicate the importance of the the resolved photon contribution to the total jet cross section and its suppression with increasing virtuality. The Q^2 dependence of the di-jet cross section and of the ratio $\sigma^{res}/\sigma^{dir}$ was shown. The first measurements of the LO effective PDF of the photon in the region $1.4 < Q^2 < 25$ GeV^2 was presented.

Acknowledgements

I thank J. Chýla and S. Maxfield for the reading of the text and for comments.

References

1. H1 Collab., C. Adloff et al., *Eur. Phys. J.* C **1**, 97 (1998)
2. H1 Collab., C. Adloff et al., *Phys. Lett.* B **415**, 418 (1997)
3. M. Drees and R.M. Godbole, *Phys. Rev.* D **50**, 3124 (1994)
4. G.A. Schuler, T. Sjöstrand *Phys. Lett.* B **376**, 193 (1996)
5. B.L. Combridge and C.J. Maxwell, *Nucl. Phys.* B **239**, 429 (1984).
6. G. D'Agostini, *Nucl. Instrum. Methods* A **362**, 487 (1995).
7. M. Glück, E. Reya, and A. Vogt *Z. Phys.* C **53**, 127 (1992)
8. M. Glück, E. Reya, and A. Vogt *Z. Phys.* C **53**, 651 (1992)

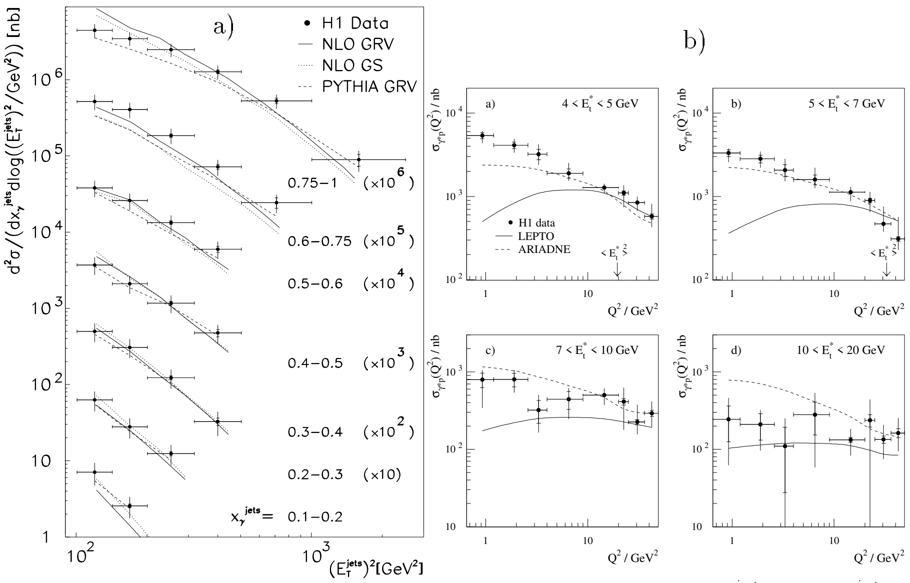

Figure 1: a) The photoproduction di-jet cross section as a function of $(E_T^{jets})^2$ and x_γ^{jets} in the range $0.2 < y < 0.83$. The data (full circles) are compared to the PYTHIA with the GRV-LO photon PDF (dashed curve) and to analytical NLO calculations with GRV-HO (full line) and GS96 (dotted line) photon PDF. b) The inclusive $\gamma^* p$ single-jet cross section as a function of Q^2 in the range $0.3 < y < 0.6$. The data (full points) are compared to LEPTO (solid line) and ARIADNE (dashed line).

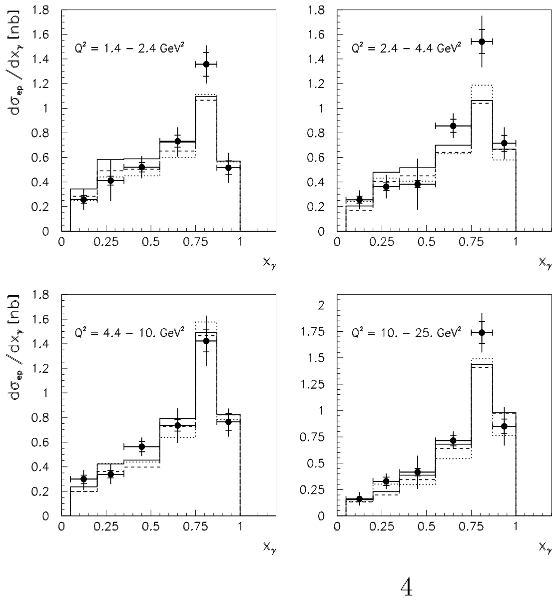

H1 Preliminary

Figure 2: The differential di-jet ep cross sections as a function of x_γ in four Q^2 intervals (points) compared to HERWIG with $\omega = 0.1, 0.05$ GeV (full, dashed line resp.) and RAPGAP with $\omega = 0.1$ GeV (dotted line) used in DG suppression function.

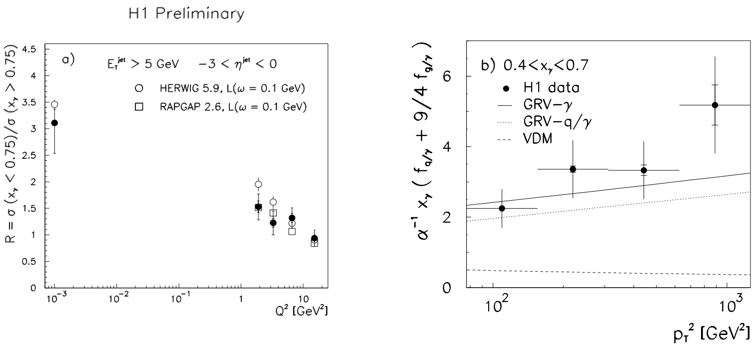

Figure 3: a) The ratio $\sigma_{res}/\sigma_{dir}$ as a function of Q^2. The data (full circles) are compared to the HERWIG (open circles) and RAPGAP model (open squares) with DG suppression for $\omega = 0.1$ GeV. b) The LO effective PDF of the photon $x_\gamma f_{\text{eff}}^{\gamma}$ normalised to the α_{em} for $0.4 < x_\gamma < 0.7$ as a function of the squared parton momentum p_T^2. The data (points) are compared to the pointlike (full curve), VDM (dashed) and quark (dotted) component of the effective GRV-LO PDF of the photon.

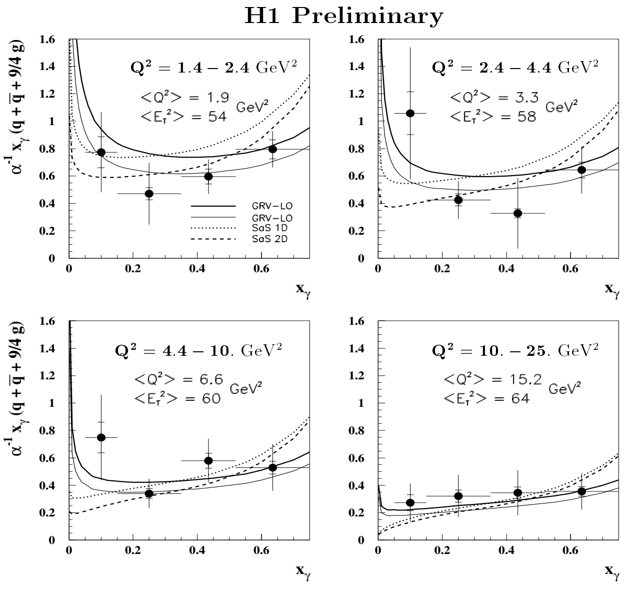

Figure 4: The LO effective parton distribution of the photon $x_\gamma f_{\text{eff}}^{\gamma}$, normalised to the α_{em}, in four intervals of the photon virtuality Q^2. The data (points) are compared to the effective PDF of the photon using the GRV-LO parametrisation multiplied by DG suppression function with $\omega = 0.1, 0.05$ GeV (full thick, full thin line resp.) and SaS1D (dotted line), SaS2D (dashed line) parametrisations.